Ultrahigh-birefringent squeezed lattice photonic crystal fiber with rotated elliptical air holes

Felipe Beltrán-Mejía,[1] Giancarlo Chesini,[2] Enrique Silvestre,[1] Alan K. George,[3] J. C. Knight,[3] and Cristiano M. B. Cordeiro[2,*]

[1]*Departamento de Óptica, Universidad de Valencia, 46100 Burjassot, Valencia, Spain*
[2]*Instituto de Física "Gleb Wataghin," Universidade Estadual de Campinas—UNICAMP, Campinas, São Paulo, Brazil*
[3]*Centre for Photonics and Photonic Materials, Department of Physics, University of Bath, Bath, UK*
**Corresponding author: cmbc@ifi.unicamp.br*

Received October 2, 2009; revised December 1, 2009; accepted January 2, 2010;
posted January 12, 2010 (Doc. ID 118064); published February 11, 2010

We report an experimental realization of a highly birefringent photonic crystal fiber as a result of compressing a regular hexagonal structure. The experimental measurements estimate a group birefringence of approximately 5.5×10^{-3} at 1550 nm in good agreement with the numerical results. We study the influence of compressing the regular structure at different directions and magnifications, obtaining a method to realistically enhance the phase birefringence while moderating the group birefringence. © 2010 Optical Society of America

OCIS codes: 060.2420, 230.4000, 060.2280, 060.2310, 060.4005.

Several applications in fiber-optics-based sensing and telecommunications systems require high-birefringent waveguiding for polarization maintaining or for breaking the degeneracy of a propagation mode. However, the polarization state of a mode propagating through a conventional fiber is random and unknown owing to environmental conditions such as mechanical stress and fabrication imperfections. This difficulty can be surpassed by breaking the fiber's symmetry (form birefringence) or by stressing the core material. Photonic crystal fibers (PCFs), optical fibers with a core surrounded by an array of air holes extending down the fiber length, have been shown to sometimes be much more birefringent than conventional fibers owing to a more complex geometry and a higher difference in the refractive index. Although there are some experimental realizations of different types of highly birefringent PCFs (Hi-Bi PCFs), most of them are based in deformations with a low degree of control during the fabrications process [1–3] or contain various elements around the core [4,5].

Recently, an appealing anisotropic PCF has shown to be potentially highly birefringent, as it has been proved by some numerical results [6,7]. Its birefringent properties relies on a regular lattice that has been squeezed in one direction, inducing an ellipticity in both the core and the air holes, as depicted in Fig. 1(a). In [6], it is shown how by augmenting the ellipticity of the holes the magnitude of both phase and group birefringence increases. On the other hand, [7] shows how by compressing a regular hexagonal lattice, the phase birefringence can be dramatically increased. In this Letter we report experimental results that are, to our knowledge, the first realization of a squeezed lattice PCF [see Fig. 1(a)].

Apart from a solid core and a microstructured cladding, the fiber presents two external air holes [8]. Playing with differential pressure between the cladding and external holes it is possible to adjust the compression factor K ($0<K\leqslant100\%$, being $K=100\%$ the undeformed structure whose birefringence is null) and the holes' ellipticity. The angle, θ, between the vertices of the hexagon [see Fig. 1(b)] and the line that links both external holes (shown by arrows) can be controlled by rotating the internal structure during the stacking procedure. As expected, these deformations from a regular lattice with circular air holes break the fiber symmetry inducing a birefringence. The fiber shown in Fig. 1(a) presents $K\approx60\%$, $\theta\approx20°$, and B_g around 5.5×10^{-3} at 1550 nm. This fiber was pulled by pressurizing the cladding holes (22 kPa) and the two external holes (7 kPa). The experimental measurements done suggest this fiber has a monomode behavior (or at least nominally

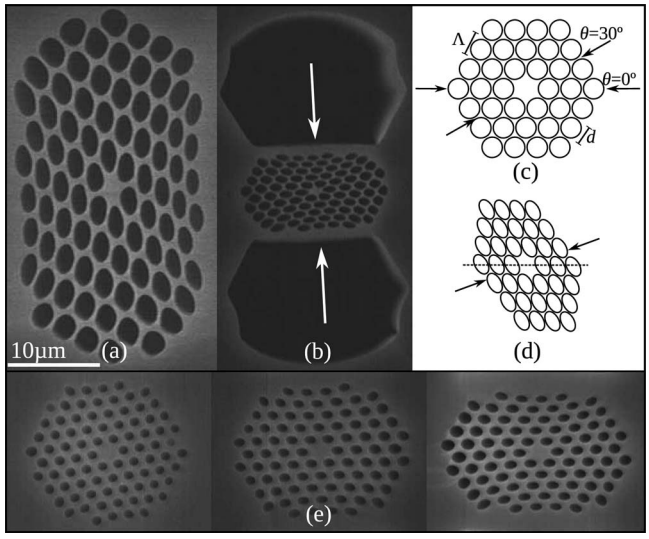

Fig. 1. (a) Detailed scanning electron microscope (SEM) image of an elliptical core Hi-Bi fiber. Note the effect of the lateral stress. (b) Hi-Bi fiber deformed by compressing approximately up to a 60% of its original size along an angle $\theta=20°$ with respect to a major diagonal of the undeformed hexagon. (c) Regular structure before the deformation. Arrows show the compression direction with respect to the horizontal axis. (d) Structure compressed in the direction shown by the arrows. (e) Set of three other fibers constructed with different compression factors.

monomode [9]) in the observed wavelength range. Figure 1(e) shows a set of three other fibers, all of them with compression angles close to 30°, fabricated by keeping the same pressure on the cladding holes (18 kPa) but increasing the applied pressure in the external holes from 0 to 6 kPa.

This work includes a numerical study around the compression of the fiber at different directions. We find out that compressing normally to a side of the hexagon [$\theta=30°$ in Fig. 1(c)] gives a more uniform overall compression than compressing through the vertices, as it has been done in previous numerical works ($\theta=0$) [6,7,10]. In Fig. 1(b) it is shown how the structure is askew relative to the two big compressing air holes; in this way it is possible to compress the fiber through an arbitrary angle θ. Since an hexagonal regular structure has a sixfold symmetry and also exhibits several mirror reflection planes, it is only necessary to analyze the compressed structures in the range $0 \leqslant \theta \leqslant 30°$. Note that the direction of compression, θ, determines both the rotation of the elliptical air holes and the direction at which the lattice is squeezed. This also causes a stress parallel to a face of the hexagon that deforms the regular structure, as illustrated in Fig. 1(d).

Deforming a regular PCF not only increases its phase birefringence, $B_p = n_{\mathrm{eff},x} - n_{\mathrm{eff},y}$, where $n_{\mathrm{eff},\circ}$ are the effective indexes for the two fundamental polarization states, but it also increases the group birefringence, B_g, the derivative of B_p with respect to the frequency. A common misconception is to assume that the difference between B_g and B_p is negligible. However, B_g differs from B_p by a term proportional to the slope of B_p as a function of λ, like n_g does from n_{eff},

$$B_g(\lambda) = B_p(\lambda) - \lambda \partial B_p / \partial \lambda . \quad (1)$$

Previous numerical results [6] demonstrate that for compressed Hi-Bi PCFs, B_g increases along with the air-hole ellipticity. On the other hand, B_p can be significantly increased by further compressing the base lattice on the horizontal direction ($\theta=0$) [10], as defined in Fig. 1(c). The latter approach has been used to obtain very high numerical results for B_p, compressing up to levels where the fabrication process becomes prohibitive. Also, we find out that this lattice compression approach boosts B_g as well. This may be undesirable in some nonlinear applications, since B_g is closely related with the polarization mode dispersion [6].

Up to now, as it has been pointed out above, different geometrical parameters (ellipticity, compression magnitude, and direction) have been studied individually, without considering the ligatures between the different parameters and making it hard to understand the processes underlying the compression. To gain some physical insight on realistic compressed PCFs, we have started from an undeformed regular structure based on a regular hexagonal lattice with pitch $\Lambda=3.1$ μm and presenting circular air holes with diameter $d=2.8$ μm, as shown in Fig. 1(c). Then we squeeze the fiber by a factor K in a given direction defined by the angle θ [see Fig. 1(d)]. The fiber in Fig. 1(a) can be modeled using $K=61\%$ and $\theta=20°$. To calculate the dispersion relations of the two polarization states of the fundamental mode we used an iterative Fourier method [11,12] in order to evaluate B_p and B_g in a fast and accurate manner.

Figure 2 shows how B_p and B_g depend on θ for different compression factors. As shown, the maximum B_p is obtained by compressing along $\theta=0$. Several authors [13,14] have pointed out that the magnitude of B_g could be higher than B_p in fibers who exhibit a form birefringence like those presented in this Letter, as shown in Fig. 2. We also realized that the compression approach for manufacturing Hi-Bi PCFs makes B_p more dispersive, and then the magnitude of the last term of Eq. (1) increases substantially as it has been experimentally demonstrated [3]. Therefore it will be useful to find a way to tune the chromatic dispersion of B_p when the fiber is further compressed in order to decrease B_g. In Fig. 2 it is shown how, by changing the compression direction from 0 to 30° for a highly compressed PCF ($K=60\%$), both B_g and B_p decreases, but the former in a greater extent, $[B_g(30°)-B_g(0°)]/[B_p(30°)-B_p(0°)]=1.55$.

A way to reduce the wavelength dependence of B_p in a compressed Hi-Bi fiber is to choose an appropriate compression angle. Certainly, this also depends on K, as shown in Fig. 3. In this figure B_g and B_p are plotted against λ for different compression factors, showing a compromise between K and birefringence. Experimental measurements for B_g, represented by circles in Figs. 3 and 4, were done by the wavelength scanning method [15] for one of the fibers [Fig. 1(a)] that exhibits high birefringence at a nonconventional compression direction. Although the continuous lines represent idealized numerical results, a good agreement is shown compared with the experimental measurements of B_g. The compression direction $\theta=20°$ has been chosen as the approximate value in the selected fiber. The inset of Fig. 3 shows the ratio between the rotated and the nonrotated values of B_p and B_g as a function of wavelength at different compression angles. It shows how the growing ratio of B_g

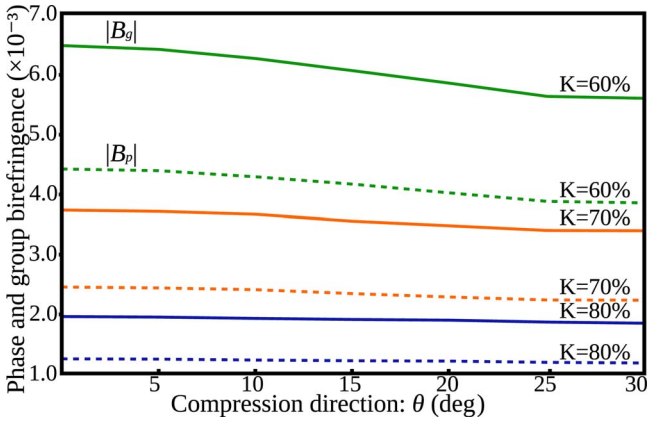

Fig. 2. (Color online) Group (solid) and phase (dashed) birefringence as a function of the compression direction (θ) at a wavelength $\lambda=1.55$ μm. For all cases $\Lambda=3.1$ μm and $d=2.8$ μm as in Fig. 1. Note that although B_p reaches a maximum for $\theta=0$, B_g is boosted more than what B_p increases.

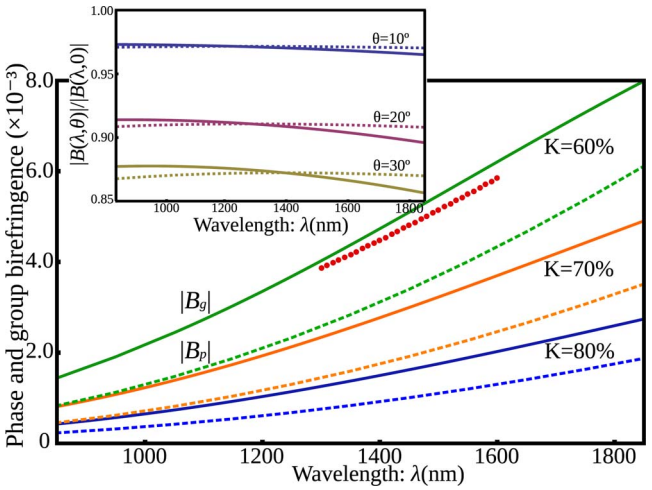

Fig. 3. (Color online) Group (solid) and phase (dashed) birefringence as a function of the wavelength for $\theta=20°$ and several compression factors. Raising the compression considerably increases the wavelength dependence of B_g. Circles correspond to experimental values for B_g, showing good agreement when $K=61\%$. In the inset, B_g (solid) and B_p (dashed) are relative to its value at $\theta=0$, versus wavelength, for $K=60\%$, and several compression directions, θ. The values of Λ and d are the same as in Fig. 2.

is reduced compared with the case of B_p when θ gets closer to 30° for wavelengths over 1400 nm.

Therefore, compressing a Hi-Bi PCF at an angle close to 30° is not only for practical reasons but it also helps in reducing B_g. Of course, as important as the compression factor and the direction, is the global magnification, M, of the structure, i.e., the factor by which Λ and d are simultaneously scaled, maintaining K and θ constant. Figure 4 shows B_g as a function of wavelength for different values of M. As can be seen from Fig. 4, the curves of B_g exhibit an inflexion point around a certain wavelength that decreases with M, in such a way that the difference of group-velocity dispersions may show a flattened behavior around these wavelengths. Further reductions may allow us to obtain flattened behaviors for B_g, and, correspondingly, the difference between the group-velocity dispersion of both polarization states will vanish.

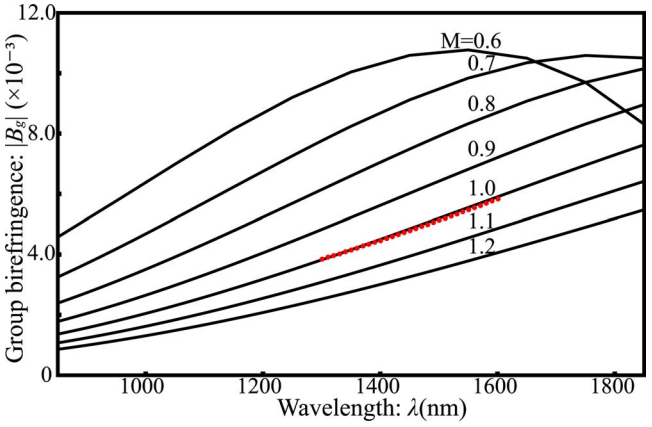

Fig. 4. (Color online) Group birefringence for different magnifications using $K=61\%$ and $\theta=20°$. The unscaled system ($M=1$) represents the structure whose geometrical parameters are closer to those measured at the fiber shown in Fig. 1(a), being the values of Λ and d, as shown in Fig. 2.

In conclusion, we have shown that a way to restrain B_g and at the same time enhance B_p is to choose the appropriate compression direction. For other configurations we have been able to obtain a relative reduction of up to the 70% for B_g relative to the nonrotated compressed fiber. Also by controlling the magnification of the structure, we can tune the wavelength at which B_g (or its derivative) shows a flattened behavior. Inspired in these results, we have been able to construct, for the first time, up to our knowledge, a compressed Hi-Bi PCF. We also have presented a new way to compress a PCF at an arbitrary direction. This compressed fiber exhibits a high B_p, while B_g is restrained.

This work has been financially supported by the Brazilian agencies FAPESP and CAPES, the Spanish Ministerio de Educación y Ciencia (MEC) and Generalitat Valenciana (grants TEC2008-05490 and PROMETEO2009-077) and the UK Engineering and Physical Sciences Reasearch Council (EPSRC). The SEM images were performed at Laboratório Nacional de Luz Síncrotron (LNLS), Brazil. F. Beltrán gratefully acknowledges financial support from MEC (grant BES-2006-12063). C. Cordeiro acknowledges helpful discussions with M. V. Andrés.

References

1. S. Kim, C.-S. Kee, J. Lee, Y. Jung, H.-G. Choi, and K. Oh, J. Appl. Phys. **102**, 016101 (2007).
2. N. A. Issa, M. A. van Eijkelenborg, M. Fellew, F. Cox, G. Henry, and M. C. J. Large, Opt. Lett. **29**, 1336 (2004).
3. A. Ortigosa-Blanch, A. Díez, M. Delgado-Pinar, J. L. Cruz, and M. V. Andrés, IEEE Photon. Technol. Lett. **16**, 1667 (2004).
4. M. Delgado-Pinar, A. Díez, S. Torres-Peiró, M. V. Andrés, T. Pinheiro-Ortega, and E. Silvestre, Opt. Express **17**, 6931 (2009).
5. A. Ortigosa-Blanch, J. C. Knight, W. J. Wadsworth, J. Arriaga, B. J. Mangan, T. A. Birks, and P. S. J. Russell, Opt. Lett. **25**, 1325 (2000).
6. M. J. Steel and J. Osgood, Opt. Lett. **26**, 229 (2001).
7. L. Zhang and C. Yang, Opt. Express **12**, 2371 (2004).
8. G. Chesini, C. M. B. Cordeiro, C. J. S. de Matos, M. Fokine, I. C. S. Carvalho, and J. C. Knight, Opt. Express **17**, 1660 (2009).
9. I. Bassett and A. Argyros, Opt. Express **10**, 1342 (2002).
10. Y. Yue, G. Kai, Z. Wang, T. Sun, L. Jin, Y. Lu, C. Zhang, J. Liu, Y. Li, Y. Liu, S. Yuan, and X. Dong, Opt. Lett. **32**, 469 (2007).
11. E. Silvestre, T. Pinheiro-Ortega, P. Andrés, J. J. Miret, and A. Ortigosa-Blanch, Opt. Lett. **30**, 453 (2005).
12. E. Silvestre, T. Pinheiro-Ortega, P. Andrés, J. J. Miret, and A. Coves, Opt. Lett. **31**, 1190 (2006).
13. S. C. Rashleigh, Opt. Lett. **8**, 336 (1983).
14. M. Legre, M. Wegmuller, and N. Gisin, J. Lightwave Technol. **21**, 3374 (2003).
15. S. C. Rashleigh, Opt. Lett. **7**, 294 (1982).